34th Annual International Conference of the IEEE EMBS
San Diego, California USA, 28 August - 1 September, 2012

Non-contact Cardiopulmonary Monitoring Algorithm for a 24 GHz Doppler Radar

Nicusor Birsan, *Member, IEEE*, and Doru-Petru Munteanu, *Member, IEEE*

***Abstract*— The paper presents the particularities of using a Doppler radar in the 24 GHz band for non-contact cardiopulmonary monitoring. To separate heart beat from respiration we looked for a pattern in time-frequency domain instead of trying to extract directly the distance from phase observation in the baseband signal. By selecting the proper components from the Gabor transform prior expansion we obtained good accuracy for heart beat and respiration rates. Also, with minor correction in frequency, the algorithm leads to usable heartbeat waveform, opening new doors for further information extraction.**

I. Introduction

Important progresses have been made in developing small and wearable sensors for vital signs monitoring, but their usage in either hospitals or homes is still rather uncommon, due to a series of reasons including discomfort, distress, movement obstruction, etc. [10]. There are also many situations when attaching these wearable sensors can be very difficult (e.g. when patients have severe burns or injuries). Non-contact monitoring devices could helps healthcare professionals in such situations by providing critical information about a patient's state, not only during the course of surgery, but also before and after a surgery is performed or even in ambulance [16]. Doppler radar remote sensing of vital signs has shown promise to be a powerful tool for health care, emergency, and surveillance applications. However, there are only few products, just for respiration monitoring reported in [6]. Although the proof of concept demonstrated for various applications, the principle has not been developed to the level of practical application, "mainly due to a lack of an effective way to isolate desired target motion from interference" [9]. Our paper proposes to fill the gap between microwave front-end and vital sign analyses with an effective signal processing method which successfully separates heart beat from respiration rate, allowing at the same time acceptable isolation from interference.

II. Doppler Radar in the 24 GHz Band

A. Human Vital Signs Detection Using Doppler Radar

As shown in Fig. 1 (a), the Doppler radar sends a continuous electromagnetic wave TX towards the patient chest where is reflected, turning back to the radar antenna as signal RX, which is the same as the transmitted signal, but delayed with a time depending on the distance between radar antenna and the target - the patient's chest. After mixing the direct signal with the received one, low pass filtering, to extract only the based-band components, and amplification we obtain two signals: in-phase and quadrature, Fig. 1(b). With such a configuration it is possible to sense the chest movements caused by respiration and heart beat. Usually a Doppler radar does not need to modulate the transmit signal, so it transmits a continuous wave single-tone signal with the frequency f. However, the oscillator is not perfect, so the signal include an inherent phase noise $\phi(t)$:

$$s_T(t) = A_{TX} \cos\left(2\pi f t + \phi(t)\right). \tag{1}$$

The signal reflected from a single target turns back to the receiving antenna with a delay $\tau = 2L/c$, the time needed for electromagnetic waves to travel two times the target distance, L, with the propagation velocity $c \cong 3 \cdot 10^8$ m/s. With these notations the received signal is:

$$s_R(t) = A_{RX} \cos\left(2\pi f \cdot (t-\tau) + \phi(t-\tau)\right). \tag{2}$$

The amplitude, A_{RX}, is also affected by the range, a dependence expressed in radar equation, but there is not a direct relationship between range and amplitude since the power of the receiving signal has a strong dependence with radar cross section (RCS). In the case of cardiopulmonary radar RCS has large variations from front to back of the patient [12]. A small part of the transmitted signal goes to a mixer where is mixed with the received signal, basically a multiply operation between the two signals. To sense if the target is approaching or departing the path is doubled by

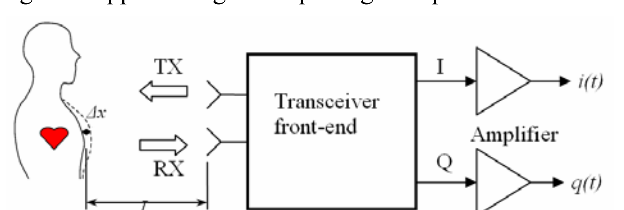

(a)

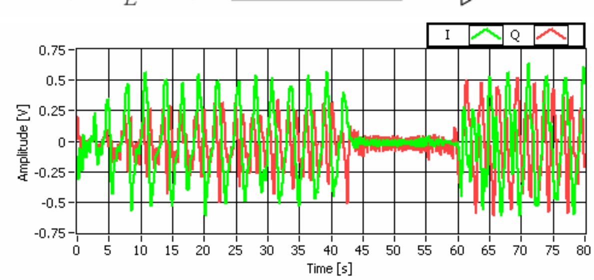

(b)

Figure 1. Block diagram of a Doppler radar for non-contact cardiopulmonary monitoring (a), and intermediate frequency signals I/Q (b).

N. Birsan was with the Military Technical Academy, Bucharest, Romania and now is with MB Telecom Ltd, Otopeni, Romania (corresponding author to provide phone: +40-728-444263; e-mail: nicusor.birsan@ mbtelecom.ro).

D.P. Munteanu is with MB Telecom Ltd, Otopeni, Romania. He also was with Military Technical Academy, Bucharest, Romania (e-mail: doru.munteanu@ mbtelecom.ro).

including two mixers, one with in-phase signal from local oscillator and one in quadrature. After filtering out the higher frequency components the mixer output consists into two intermediate frequency signals:

$$\begin{cases} i(t) = U\cos\left(2\pi f\cdot\tau + n_\phi\right) \\ q(t) = U\sin\left(2\pi f\cdot\tau + n_\phi\right) \end{cases}. \tag{3}$$

The phase noise component, $n_\phi = \phi(t) - \phi(t-\tau)$, usually affects the measurement accuracy as explained in many papers, such as [17], but, for the sake of explanation simplicity, it will be neglected. The amplitude of the two components is slight different because the signals follows two hardware paths with different gain. However, we can write the same amplitude U because the two channels can be calibrated in laboratory. With this simplification one can estimate the distance variation to a single target by measuring the phase of the complex signal I/Q, $\varphi(t) = 2\pi f\tau = 4\pi f\cdot L/c$, and then compute the range variations:

$$L(t) = \varphi(t)\cdot c/(4\pi f)\,. \tag{4}$$

Because the normal respiration rate is less than 0.8 Hz (48 respirations/min) while the heartbeat rate is between 0.8 Hz (48 beats/min) to 3 Hz (180 beats/min), the phase method can be used for differentiating the two signals with the appropriate filtering [11]. Simple experiments using two processing channels, one with a low pass filter, for respiration rate, and bandpass for heart beat give good results in laboratory conditions (e.g. signal is not affected by moving objects near the patient [11, 15]).

B. Characteristics of the Intermediate Frequency Signal

Driven by automotive industry, the advances of mm-wave radar technology allow the development of non-contact healthcare systems in the license-free industrial, scientific and medical (ISM) radio band of 24 GHz. The use of such a high frequency results into a compact size of radar, because the size of the passive and active components shrinks, and the accuracy is increasing to an optimum [14]. When the radar is working at lower frequency the phase change is small, allowing approximations between phase and the actual signal amplitude (e.g. at 2.4 GHz [8]). In the 24 GHz band the phase change is 12 radians (3.84π) for a maximum chest displacement of 12mm [4, 13]. The phase changes almost two complete period during a single inspire-expire cycle, *i(t)* and *q(t)* having many null points. This can be seen in Fig.2 (a) as on the left Q signal has two periods during a respiration cycle. Also, on the right, after second 60, the in-phase signal has two periods per respiration cycle. This results into an impossibility of measuring respiration rate by means of simple filtering, even in very good laboratory conditions. Thinks get more complicated due to multiple targets in the proximity of the measurement sensor. The I/Q signals become a sum of all targets reflections:

$$\begin{cases} i_N(t) = \sum U_i\cos\left(2\pi f\cdot\tau_i + n_{\phi_i}\right) + I_{off} \\ q_N(t) = \sum U_i\sin\left(2\pi f\cdot\tau_i + n_{\phi_i}\right) + Q_{off} \end{cases}. \tag{6}$$

(a)

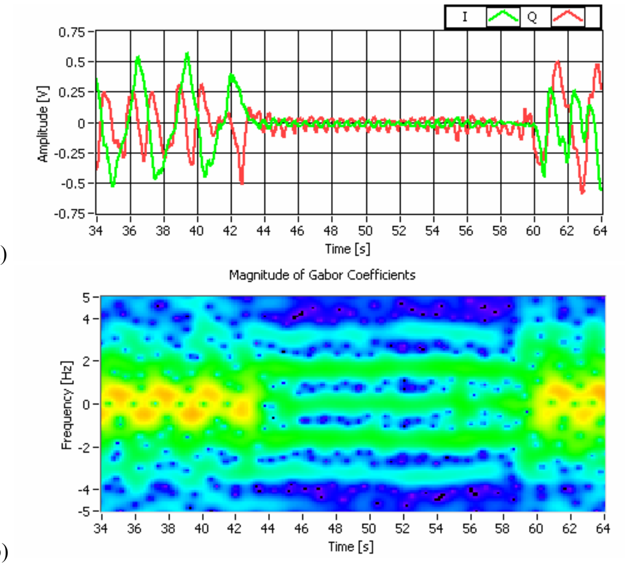

(b)

Figure 2. Detail of a signal showing a large region with holding breath (a) along with the corresponding Gabor coefficients (b).

The offset components, I_{off} and Q_{off}, are caused by the entire analog processing chain (from mixer to amplifier), plus static targets in front in front of antennas. By considering the chest as the target of interest and summing all other target' contributions as *IF* and *QF* then:

$$\begin{cases} I(t) = U\cos\left(2\pi f\cdot\tau + n\phi\right) + IF(t) \\ Q(t) = U\sin\left(2\pi f\cdot\tau + n\phi\right) + QF(t) \end{cases}. \tag{7}$$

If the *IF* and *QF* components would be filtered out then the target displacement could be measured by monitoring the phase, as explained above. Notice that if the target is moving with a constant speed (*V*) then the phase change linearly and the radar will receive the Doppler frequency $f_D = 2V\cdot f/c$ (at 24 GHz it will be 160 Hz for each m/s).

To separate the vital signs from the acquired signal we looked to cancel the *IF* and *QF* components from (7), keeping only necessary information, which contains many frequency components due to the micro-Doppler effect [2].

III. Experimental Setup and Observations

To demonstrate the new signal processing method we built experimental radar using a K-MC3 transceiver from RFbeam [19], and a 30Hz low pass 4-th order Butterworth filter with a 20dB gain. The amplified I/Q signals were acquired at 2 KSPS using a NI-USB6212 data acquisition board, controlled graphically from LabVIEW which allows further digital signal processing and presentation [18]. The higher sample rate than required allowed us to keep a low order for the analog filter, and low cost along with better pairing between the two channels. Then, as a first step in digital processing, the signal is decimated down to 200 KSPS with antialiasing filter of 120 dB. The approach also helps to improve the rejection of main supply (50 Hz in Europe).

A comprehensive synthesis of the signal processing methods can be found in [9], previous work focused into accuracy of direct measurement distance between antennas and chest [5-8]. Instead of following these methods, we

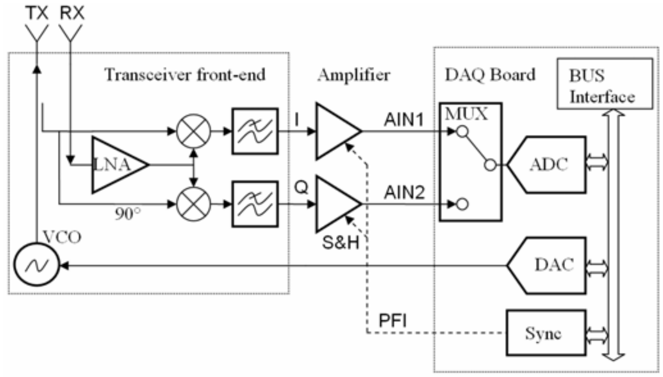

Figure 3. Block diagram of the experimental setup.

rather tried to reveal the signature of the heart beat signal in time-frequency domain. The approach is based on a simple observation: an electrocardiogram (ECG) has a short pulse during the QRS complex which corresponds to a fast move of the chest, with a velocity estimated to about 60 mm/s. Due to the Doppler effect this velocity translates into higher bandwidth signal of about 10 Hz for a 24 GHz carrier frequency. Since 10 Hz is much higher than respiration rate the system provides a better separation between heartbeat and respiration. The algorithm will work better for higher frequency bands, but it is not useful for lower bands (e.g. 2.4 GHz). We performed a time-frequency analysis by computing the short time Fourier transform (STFT) of the acquired complex signal. The component n from the m time frame window of the digitized signal s is:

$$c_{m,n} = \sum_i s_i w^*_{i-m\cdot\Delta_M} \exp(-j\cdot 2\pi \cdot n \cdot i / N)\,. \qquad (11)$$

where Δ_M is the time step.

The analysis window w in (11) is Gaussian to achieve the best time-frequency product among all the possible window functions [3]. An STFT using a Gaussian window function is sometimes called the Gabor transform.

As reported in [1], to identify the frequency components for heartbeat we acquired signals from a volunteer at a distance of 50cm while he was holding his breath. The magnitude of Gabor coefficients showed components between 8÷12 Hz. Also, there are peaks at about 6Hz which can be associated with P and T waves, slower than the QRS complex. However, the components can be seen in Fig. 4 (a) in the first two seconds. Based on those observations we selected only coefficients between 8÷12 Hz and 5÷7 Hz, and compute the Gabor expansion using a synthesis window h is:

$$\tilde{s}_i = \sum_{m=0}^{M-1}\sum_{n=0}^{N-1} \tilde{c}_{m,n} \cdot h_{i-m\Delta_M} \exp(j\cdot 2\pi \cdot n \cdot i / N)\,. \qquad (12)$$

where: $\tilde{c}_{m,n} = \begin{cases} c_{m,n} & \text{for } n \text{ in the selected bands} \\ 0 & \text{for n outside selected bands} \end{cases}$

Of course, the expansion of only high frequency components results into a high frequency signal. To count the real heart beats the resulted signal is then low filtered. The output looks like in Fig. 4 (c), which is very similar with an ECG. This means a monitoring system can be easily built for running in real time a simple algorithm: acquire a signal window, compute Gabor transform, select coefficients and Gabor expansion to get a displayable waveform.

IV. Monitoring Algorithm

The algorithm for heartbeat monitoring was already described above. Anyway, the chest movement caused by respiration affects the components selected for expansion. Also, we were unable previously to extract the respiration rate directly from time-frequency analyses because we used the optimum variance for Gaussian window [1]. By reducing the variance we get a higher frequency resolution at the same time resolution. This way, inspire and expire periods are clearly separated, as in Fig. 4(a), and can be marked by the position of the peak magnitude in each time frame, Fig. 4(b). The chest is moving towards radar during inspire and vice versa, resulting different frequency sign. The respiration affects all heartbeat frequency components. After the peak bin has been identified in each frame then all components can be corrected. In Fig. 5 (a) the heartbeat pulse from second 5 is missing. If all components from a time frame are translated

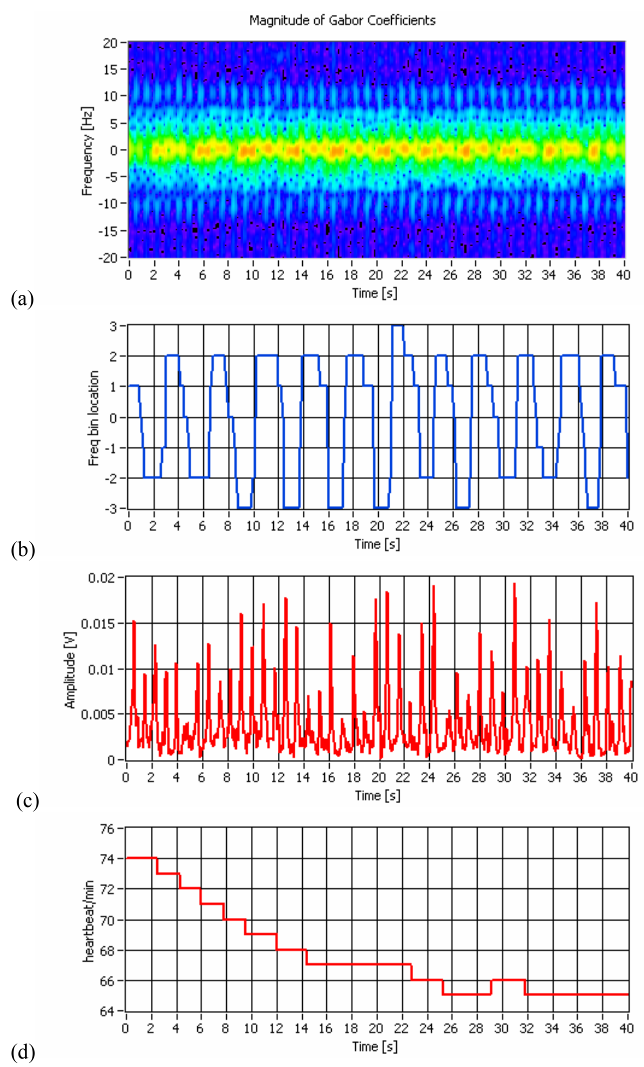

Figure 4. Magnitude of Gabor coefficients (a), respiration signal (b), heartbeat signal (c), and heartbeat variability (d).

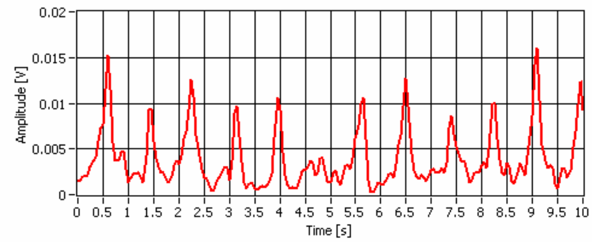

(a)

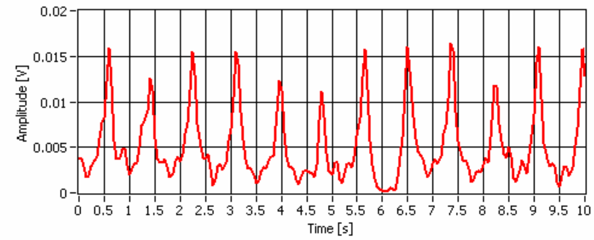

(b)

Figure 5. Restored heart beat without correction (a), and after correction in time-frequency domain (b).

prior Gabor expansion then the pulse is "restored". Actually, the waveform in Fig. 5 (b) can be used for simple counting of heartbeats without errors. The method is successful for small patient movements too. However, rejecting other target movements, including patient's head or arms is still demanding further research.

Resuming, the proposed monitoring algorithm for non-contact monitoring consists into: acquire I/Q signal; compute de Gabor transform; determine frequency bins for maximum peak in each time frame; count transitions from negative to positive frequency as respiration rate; correct frequency bin location for all coefficients in a time frame; Gabor expansion on selected components; filter the Gabor expansion result; count heartbeats or perform heartbeat variability analyses as in Fig 4 (d). Optionally, the system may determine the actual distance to the patient chest using multiple frequencies or using a frequency shift keying on the transceiver oscillator, as described in [1]. The actual monitoring algorithm will start only if there is a target within a predetermined range (e.g. 50-100 cm). For this purpose, in our experimental the analog output from the data acquisition board controls the voltage controlled oscillator, and the amplifier uses a sample and hold circuit synchronized with acquisition through a programmable function interface signal (PFI).

V. Conclusion

The algorithm described in the paper was successfully tested using the experimental setup on a large number of volunteers with good accuracy. Further research is needed to find the best fit pattern for the vital signs in time-frequency domain. This will lead to a better separation from the other micro-Doppler effects which are inherent in a normal monitoring environment such as in home, hospital or ambulance.

After a continuous refinement, the monitoring algorithm became simple enough to be implemented into a low cost monitoring device. Also, the latest advances in processing architectures dimmed the frontier between microcontrollers and digital signal processors (DSP), the former borrowing DSP functions. Gabor transform is basically a STFT which is implemented today for low cost microcontrollers, such as ARM Cortex-M3, or even more suitable, Cortex-M4F with floating point coprocessor. By using LabVIEW for refining algorithms it will be easy to port algorithms for ARM targets (e.g. Stellaris from Texas Instruments).

References

[1] N. Birsan, D.P. Munteanu, G. Iubu, T. Niculescu., "Time-frequency analysis in Doppler radar for noncontact cardiopulmonary monitoring", *in Proc. of IEEE International Conference E-Health and Bioengineering – EHB 2011*, 3rd Edition, Iasi, Nov. 2011, pp. 1-4

[2] V.C. Chen, F Li, S Ho, H Wechsler, "Micro-doppler effect in radar phenomenon, model and simulation study", *IEEE Trans on AES*, 42 (1) 2006, pp 2 – 21

[3] V.C. Chen and H. Ling, *Time-Frequency Transforms for Radar Imaging and Signal Analysis*, Artech House, Norwood, 2002

[4] A. De Groote, M. Wantier, G. Cheron, M. Estenne, and M. Paiva, "Chest wall motion during tidal breathing", *Journal of Applied Physiology* (1997), vol. 83, no. 5, pp. 1531-1537

[5] A.D. Droitcour, O.B. Lubecke, V.M. Lubecke, J. Lin, G. Kovacs, "Range correlation and I/Q performance benefits in single-chip silicon Doppler radars for noncontact cardiopulmonary monitoring", *IEEE Trans. Microwave Theory Tech.*, vol. 52, Mar, 2004 , pp.838-848

[6] A.D. Droitcour, et al., "Non-contact respiratory rate measurement validation for hospitalized patients", *in Proc. of Annual Int. Conf IEEE Eng Med Biol Soc*, *EMBC 2009*, Sept. 2009, pp. 4812 - 4815

[7] R. Fletcher, and J. Han. "Low-cost differential front-end for Doppler radar vital sign monitoring", *Microwave Symposium Digest*, 2009, pp. 1325-1328

[8] E.F. Greneker, "Radar sensing of heartbeat and respiration at a distance with applications of the technology", *in Proc. IEEE Radar Conf.*, 1997, pp. 150-154

[9] A. Host-Madsen, et al., "Signal processing methods for Doppler radar heart rate monitoring," in D. Mandic et al (Eds): *Signal Processing Techniques for Knowledge Extraction and Information Fusion*, Springer-Verlag, Berlin, 2008

[10] R. Ichapurapu, et al., "A 2.4 GHz non-contact biosensor system for continuous vital-signs monitoring",*10th Annual IEEE Wireless and Microwave Technology Conference (WAMICON '09)*, April 2009

[11] J.G. Kim, S. Sim, S. Cheon, S. Hong, "24 GHz circularly polarized Doppler radar with a single antenna", *European Microwave Conference*, Paris 2005, pp.1383-1386

[12] J.E. Kiriazi, O. Boric-Lubecke, V.M. Lubecke, "Radar cross section of human cardiopulmonary activity for recumbent subject", *in Proc. of Annual Int. Conf IEEE Eng Med Biol Soc*, *EMBC 2009*, Sept. 2009, pp. 4808 - 4811

[13] T. Kondo, T. Uhlig, P. Perberton, and P. D. Sly, "Laser monitoring of chest wall displacement," *European Respiratory Journal*, vol. 10, 1997, pp. 1865–1869

[14] C. Li, Y. Xiao, J. Lin, "Optimal carrier frequency of non-contact vital sign detectors", *in Proc. of IEEE Radio and Wireless Symposium*, January 2007, pp. 281-284

[15] O. Postolache, P.M. Girao, E.C. Pinheiro, G. Postolache, "Unobtrusive and Non-invasive Sensing Solutions for on-line Physiological Parameters Monitoring", in A. Lay-Ekuakille, S.C. Mukhopadhyay (Eds), *Wearable and Autonomous Biomedical Devices and Systems for Smart Environment*, Springer, Berlin, 2010

[16] S. Suzuki et al., "A non-contact vital sign monitoring system for ambulances using dual-frequency microwave radars", *Medical and Biological Engineering and Computing*, vol 47, Springer Berlin, 2009, pp 101-105

[17] Wu, T., X. Tang, and F. Xiao, "Reserch on the coherent phase noise of millimeter-wave doppler radar", *Progress In Electromagnetics Research Letters*, Vol. 5, 2008, pp 23-34

[18] Z. Zeng-rong, B. Ran, "A FMCW radar distance measure system based on LabVIEW", *Journal of Computers*, Vol. 6, No. 4, April 2011, pp.747-754

[19] K-MC3 Radar Transceiver, www.rfbeam.ch/products/k-mc3-transceiver/, acc. March, 2012